DOI: 10.3901/CJME.2013.06.1243, available online at www.cjmenet.com; www.cjmenet.com.cn

Experimental Study on Wear and Spalling Behaviors of Railway Wheel

WANG Wenjian, GUO Jun, and LIU Qiyue*

Tribology Research Institute, Southwest Jiaotong University, Chengdu 610031, China

Received June 21, 2012; revised August 5, 2013; accepted August 23, 2013

Abstract: The current researches of the wear and spalling behaviors of wheel/rail materials focus on the field investigation rather than the mechanism. However, it is necessary and significant for clarifying the mechanism and relationship between the wear and spalling damage of railway wheel to test and reproduce the wheel damages in laboratory. The objective of this paper is to investigate the wear and spalling damage behaviors of railway wheel using a JD-1 wheel/rail simulation facility, which consists of a small wheel serving as rolling stock wheel, and a larger wheel serving as rail. The damage process of wheel roller is explored in terms of the creep ratio, axle load, and carbon content by means of various microscopic examinations. The experimental results show that the wear volume growth of wheel roller is proved to be proportional to the increase of the creep ratio and normal load between simulating wheel and rail. The increase of carbon content of wheel material causes a linear reduction in the wear volume. The microscopic examinations indicate that the rolling wear mechanism transfers from abrasive wear to adhesive and fatigue wear with an increase of tangential friction force, which results in the initiation of fatigue crack, and then aggravates spalling damage on the wheel roller surface. The surface hardness of material depends strongly upon its carbon content. The decrease of the carbon content of wheel material may alleviate spalling damage, but can cause a significant growth in the wear volume of wheel roller. Therefore, there is a competitive relationship between the wear and spalling damage of wheel material. This research proposes an important measure for alleviating or preventing the wear and spalling damage of railway wheel material.

Key words: wear, spalling, content carbon, railway wheel, wear mechanism

1 Introduction

Considering a number of criteria, such as speed, capacity and environment, railway is a superior means of transportation. In general, the speed of passenger trains and the tonnage of freight trains are often raised to increase the efficiency of rail transport. However, wear and rolling contact fatigue (RCF) of wheel/rail would become more and more severe[1]. A variety of damages happen on railroad wheel, which mainly result from the wear of tread and flange, the scratch of tread, shelling, spalling, thread checking, and so on. It is found that spalling becomes one of the typical kinds of damages of railroad wheelset due to the increase of the speed of railway. Therefore, spalling properties have been focused on by many researchers[2–6].

Spalling is described as the loss of relatively large pieces of wheel tread material. According to AAR's (American Association of Railway) research, spalling is the result of wheel sliding which produces enough high temperature on the tread skin to metallurgically transform a thin surface layer to a different steel structure[2]. Tread defects as a result of spalling cause many spots on the wheel tread, and then an out-of-round condition appears. The out-of-round wheels cause high impact loads on the rail, which also are transmitted to the roller bearing. Moreover, these impacts maybe shorten the life of these components and affect the safety of railways and the comfort of passengers. In addition, spalling may also result in many noises between wheel and rail, and accelerate the wear of other parts.

The researches indicate that the occurrence of spalling is correlated with the contact stress of wheel/rail system, friction force, material of wheel/rail, axle load, thermal stress, structural stress, and so on[6–8]. Therefore, it is very important to develop new materials used for high speed railway wheel. At present, reducing the carbon content of steel and alloying are often used to prevent from forming the martensite layer during the sliding of wheel, and alleviate the wear and spalling of wheel/rail material.

To some extent, the more the details of spalling mechanism are known, the more the preventative measures could be developed. However, only a few works have been carried out in this field nowadays[9]. It is necessary for clarifying the mechanism of damage to test and reproduce the wheel damages in laboratory. Simulation methods for reproducing some damages of wheel/rail on test stands are classified into three: running tests on the test track, rolling contact tests wheels and circular rails-to-be of actual size, and rolling contact tests using small size cylindrical

* Corresponding author. E-mail: liuqy@swjtu.cn

This project is supported by National Natural Science Foundation of China(Grant No. 51174282), Innovative Research Teams in Universities of China(Grant No. IRT1178), and Autonomous Research Project of State Key Laboratory of China(Grant No. TPL1301)

specimens. The running tests on the test track require tremendous expenditures and time. However, simulation test using small size specimens is a cost-effective and convenient research technique.

In this paper, a JD-1 wheel/rail simulation facility is used to investigate the effects of the creep ratio, axle load and carbon content of wheel material on the wear and spalling characteristics of railway wheel. Particularly, the wear mechanism and spalling damage of railway wheel are explored in detail.

2 Experimental Details

2.1 JD-1 wheel/rail simulation facility

All experiments are carried out on a JD-1 wheel/rail simulation facility[10], as shown in Fig. 1. The tester is composed of a small wheel roller serving as rolling stock wheel (called as "simulating wheel") and a larger rail roller serving as rail (called as "simulating rail"). The diameters of the wheel and rail rollers are 200 mm and 1 070 mm, respectively. Simulating wheel and rail are driven by DC motors A and B, respectively. The power imposed on simulating wheel and rail rollers can be controlled accurately, by which traction or brake force is realized upon the simulating wheel roller.

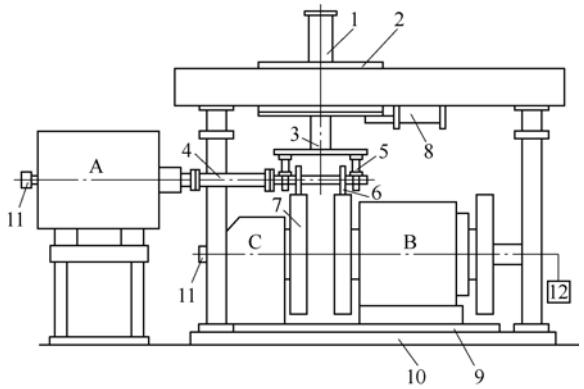

Fig. 1. JD-1 wheel/rail simulation facility

1. Normal loading cylinder; 2. Loading carriage; 3. Spindle and yoke; 4. Universal shaft; 5. 3D load sensor; 6. Simulating wheel; 7. Simulating rail; 8. Lateral loading cylinder; 9. Turning plate; 10. Base plate; 11. Optical shaft encoder; 12. Speed measuring motor; A, B. ZQDR-204 DC motor; C. Gear box

The geometric sizes of simulating wheel and rail rollers are determined by means of the Hertz simulation rule as follows:

$$(q_0)_{\text{lab}} = (q_0)_{\text{field}}, \tag{1}$$

$$\left(\frac{a}{b}\right)_{\text{lab}} = \left(\frac{a}{b}\right)_{\text{field}}, \tag{2}$$

where $(q_0)_{\text{lab}}$, $(q_0)_{\text{field}}$ are the maximum contact stresses in the laboratory and in the field, respectively; $(a/b)_{\text{lab}}$, $(a/b)_{\text{field}}$ are the ratios of semi-major axis to semi-minor axis of the contact ellipses between the wheel and rail in the laboratory and field, respectively. The schema of geometric size calculated by the above formulas is shown in Fig. 2.

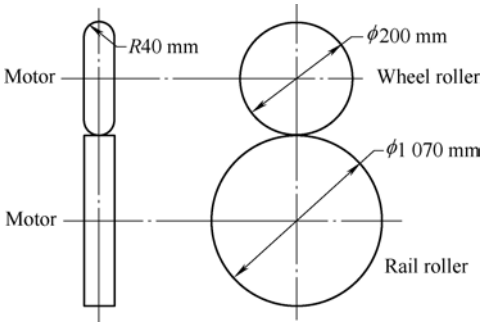

Fig. 2. Scheme size of simulating wheel and rail

The creep ratio of simulation tester is defined by the following formula:

$$\lambda = \frac{\omega_{\text{w}} R_{\text{w}} - \omega_{\text{r}} R_{\text{r}}}{\omega_{\text{w}} R_{\text{w}}} = 1 - \frac{\omega_{\text{r}} R_{\text{r}}}{\omega_{\text{w}} R_{\text{w}}} = 1 - 5.35i, \tag{3}$$

where λ is the ratio of creep between the simulating wheel/rail; ω_{w} and ω_{r} are rotating speeds of wheel roller and rail roller, respectively; R_{w} and R_{r} are the radius of wheel roller and rail roller, respectively; i is the speed ratio, equal to $\omega_{\text{r}}/\omega_{\text{w}}$. Different ratios of rotational speed can be obtained and maintained by varying exciting current of DC motors A and B (Fig. 1) throughout the test. Subsequently, the creep ratio of this tester changes from −7.5% to 7.5%.

A peculiar measurement is taken to determine the wear of wheel roller in our research. Before testing, a special mark is made on the wheel roller surface in order that the wear scar is measured at the same position each time. Polypropylene is used to copy the profile of the wear surface on the specimens before and after testing. Then the copies are examined using a high sensitive surface profilometer (TALYSURF6, England) in order to get the wear volume of either wheel roller. The wear is determined from the difference between the original profile and the wear profile (Fig. 3).

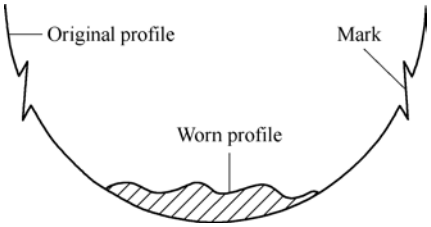

Fig. 3. Scheme of wear volume measurement

2.2 Experimental parameters and materials

Tests are conducted on the base of Hertz simulation rule. The maximum Hertzian contact stress q_0 can be calculated

by the following formulas[10]:

$$q_0 = \frac{3p}{2\pi ab}, \tag{4}$$

$$a = \alpha \sqrt[3]{\frac{3p}{4A} \cdot \eta}, \tag{5}$$

$$\eta = \frac{1-\mu_1^2}{E_1} + \frac{1-\mu_2^2}{E_2}, \tag{6}$$

$$A = \frac{1}{2}\left(\frac{1}{R_{w1}} + \frac{1}{R_{w2}} + \frac{1}{R_{r1}} + \frac{1}{R_{r2}}\right), \tag{7}$$

where p is the normal load; a and b are the lengths of semi-major axis and semi-minor axis of the contact ellipses; E_1, E_2, μ_1, μ_2 are the Young's modulus and Poisson's ratio of wheel and rail material, respectively; A is the equivalent geometric radius of wheel and rail; $R_{w1}, R_{w2}, R_{r1}, R_{r2}$ are the radius of principal curvature of wheel and rail contact point, respectively. According to Eqs. (4)–(7), Eq. (1) is rewritten as

$$p_{lab} = \left(\frac{A_{field}}{A_{lab}}\right)^2 p_{field}, \tag{8}$$

where p_{lab}, p_{field} are the normal loads in the laboratory and in the field, respectively. The normal loads calculated by Eq. (8) in the laboratory are about 2 400 N, 2 800 N, 3 200 N, which are correlative to the actual axle loads of 24 t, 28 t, 32 t, respectively. The cycle numbers of simulating wheel is 2.5×10^5 and the rotational velocity of rail roller is about 90 r/min. The creep ratios are −7.5%, −3.7%, 0, 5.7%, respectively.

The wheel roller and rail roller are made of real wheel and rail steels, respectively. Their chemical compositions in weight percentage is given in Table 1.

Table 1. Chemical composition of wheel and rail steels %wt

Specimen	C	Mn	Si	S	P
Wheel roller	0.40–0.70	0.80–1.00	0.30–0.50	≤0.045	≤0.04
Rail roller	0.62–0.77	1.35–1.65	0.15–0.37	≤0.050	≤0.04

All the tests are carried out in the ambient condition (temperature: 18–23℃, relative humidity: 50%–70%) without any lubricant. The contact surfaces are cleaned carefully with acetone before testing. A new wheel roller is used for every test and the rail roller is used repeatedly. After each test, the surface of rail roller is cut clearly using the machine tool for preventing plastic deformation from previous tests. Wear scars are examined and analyzed by various microscopic examinations including microhardness tester (MVK–H21, Japan), optical microscopy (OM) (OLYMPUS BX60M, Japan), laser confocal scanning microscopy (LCSM) (OLYMPUS OLS1100, Japan), scanning electronic microscopy (SEM) (QUANTA200, FEI, England).

3 Results and Discussion

3.1 Effect of creep ratio

The variations in the wear volume of wheel roller, as a function of the number of cycles of wheel roller at different normal loads and creep ratios, are shown in Fig. 4(a). It should be noted that the traction behavior occurs accompanied by positive creep ratio values, corresponding to the braking process in the wheel/rail system accompanied by negative creep ratio values. It is found that the wear volume increases rapidly at the beginning of testing. With increase in test time, intensive deformation happens both on the surface and on the subsurface layer of the materials during the process of wear. As a result, a state of elastic shakedown comes into being[11]. So, the wear volume increases slowly and it presents a stable wear process. Furthermore, it is observed that the wear volume of wheel roller increases with increasing in normal load and creep ratios. Fig. 4(b) shows the wear volume versus the creep ratio at the normal load of 2 400 N after 2.5×105 cycles of wheel roller. A U-shaped curve is found with a minimum at λ=0. The wear volume decreases linearly with the creep ratio increasing from −7.5% to 0, and then increases with the creep ratio increasing from 0 to 5.7%. So, the higher creep ratio aggravates wear behavior between wheel and rail contact surfaces.

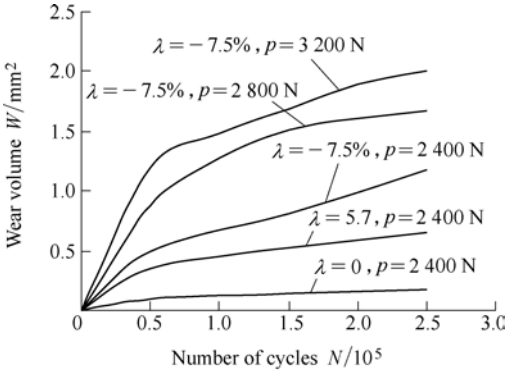

(a) Variations of wear volume as function of number of cycles of wheel roller

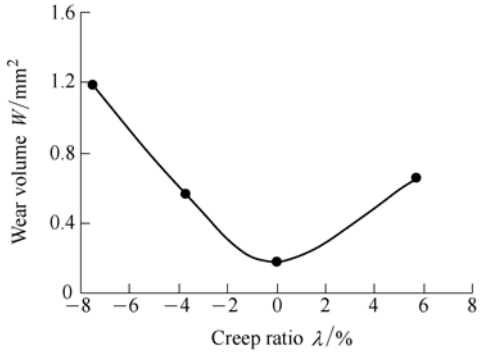

(b) Variation of wear volume as function of the creep ratio (p=2 400 N)

Fig. 4. Wear volume of wheel roller (C-0.6%)

Macro-pictures and further LCSM micrographs show the damage on the rolling surfaces of wheel roller, as shown in Fig. 5. It is seen that slight damage appears under the free rolling (λ=0), and the worn surface of the wheel is characterized by slight scratches (Fig. 5(a)). When the traction or braking force is imposed, the creep ratio decreases from 0 to −3.7% and the wear is aggravated (Fig. 5(b)). It is found that the width of wear scar is much bigger at λ=−3.7% than that at λ=0 (Fig. 5(b)), and slight delamination appears on the worn surface. With the creep ratio further increasing, massive delamination and loss of large pieces of wheel roller material, which is defined as spalling, are observed on the rolling contact surface at λ=−7.5% (Fig. 5(c)).

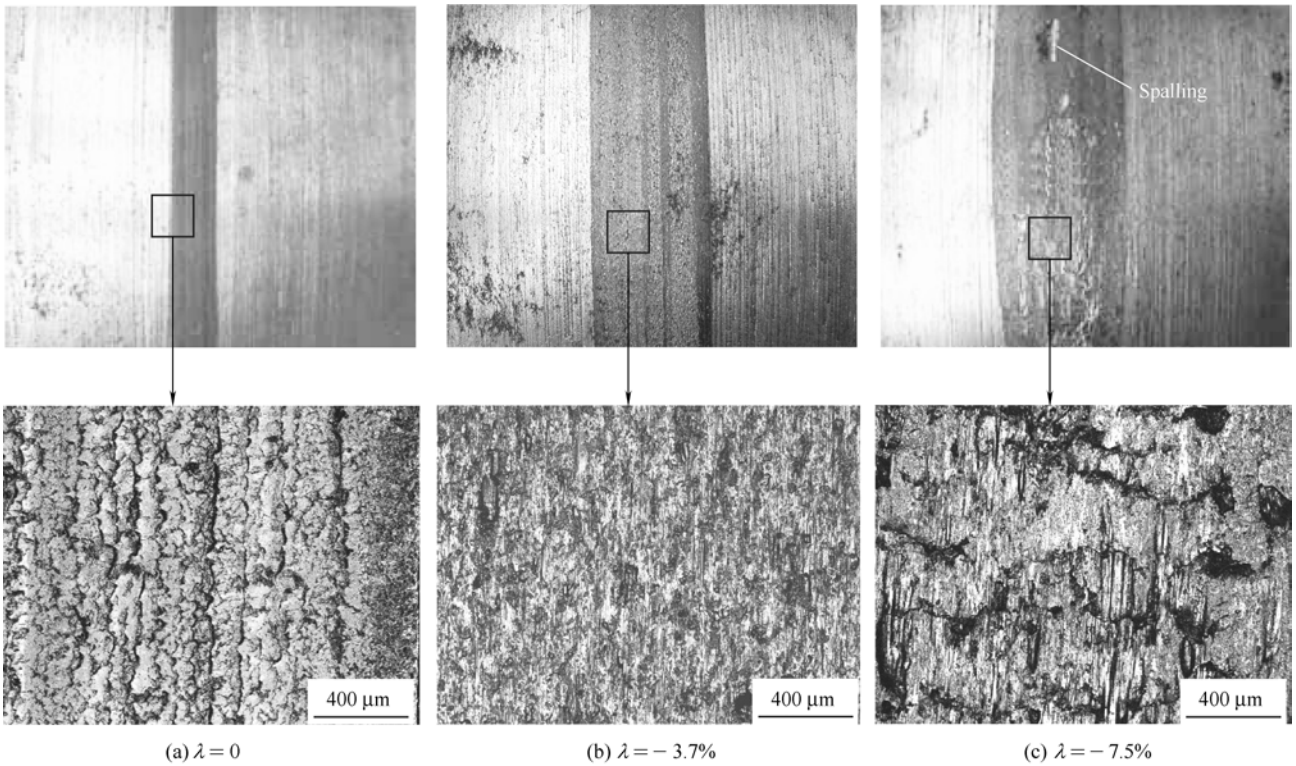

Fig. 5. Examinations of wear scar of wheel roller (C-0.6%)

Further examinations on wear scars (Fig. 5) indicate that the wear mechanisms of wheel material vary with the creep ratio. When the creep ratio is zero, tribo-oxidation and abrasive wear are dominant on the worn surface, and the hard debris staying in the contact area could result in ploughing on the worn surface (Fig. 5(a)). As we known, the damage belongs to high-cycle fatigue under pure rolling condition. With the creep ratio increasing, the worn surface is characterized by delamination, fatigue and spalling (Figs. 5(b) and 5(c)). The surface damages mainly result from fatigue and adhesive wear. Previous researches also indicated that the damage process of material has a close relation to its wear mechanism[12–13].

The curves in Fig. 4 show that the creep ratio plays an important role in the wear of the wheel roller. When the creep ratio is zero (without either traction or brake force), the tangential friction force between wheel and rail is really low, and therefore no obvious wear occurs (Fig. 5(a)). When the traction or braking force is increased, sliding takes place between wheel and rail, which causes rapid increases in both the tangential friction force and the temperature on the contact surface[12]. Therefore, significant wear and fatigue damage occur, and obvious plastic deformation as well as white layer (a different steel structure) is observed on the cross-section (Fig. 6(a)). Because the white layer is brittle and very hard, some delamination could easily happen on the worn surface. On the other hand, the maximum shear stress mainly occurs on the contact surface which is increased due to large friction force[11]. As a result, rolling contact fatigue cracks would be initiated and propagated easily (Fig. 6(b)), and finally spalling damage takes place as a result of tribo-fatigue process.

3.2 Effect of normal load

As a result of the increase of normal load from 2 400 N to 3 200 N, it is obvious that the increase of normal load leads to an almost proportional growth of the wear volume of wheel roller, as shown in Fig. 7. With the normal load increasing, the wear of wheel roller becomes more and more severe because of more large-delamination at higher normal load. So, the spalling damage is obviously aggravated on the wear surface of wheel roller at p=3 200 N (Fig. 8). It is observed in Fig. 7 and Fig. 8 that the increase of normal load not only leads to a linear increase in wear volume but also aggravates the damage of wheel roller. So, it is also found that the occurrence of spalling damage is related to the normal load.

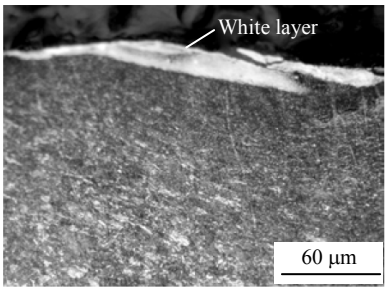

(a) White layer and plastic deformation

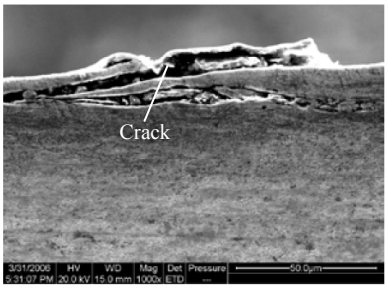

(b) Fatigue crack

Fig. 6. OM micrographs of transverse section of wheel roller (λ=−7.5%, p=2 400 N)

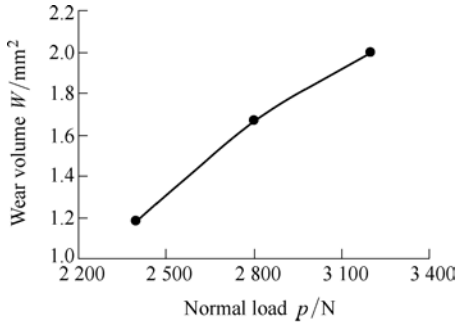

Fig. 7. Variation of wear volume of wheel roller as function of normal load (C-0.6%)

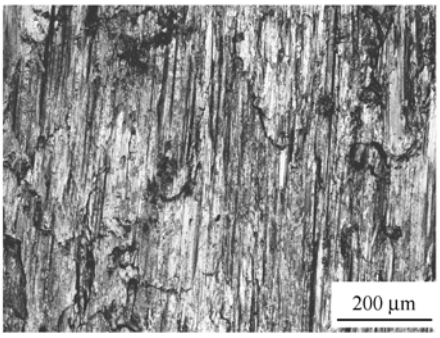

(a) p=2 400 N

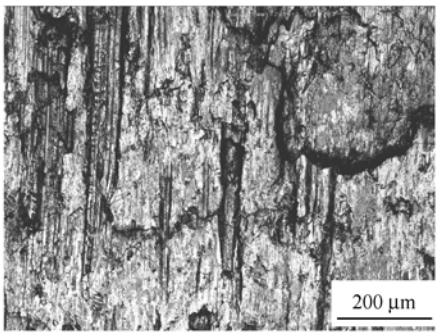

(b) p=3 200 N

Fig. 8. LCSM micrographs of wear scar of wheel roller (C-0.6%)

3.3 Effect of carbon content

Fig. 9 gives the rolling contact surfaces hardness (RCSH) with different carbon contents before and after testing. The pre-test and post-test RCSH are measured 10 times and all deviations do not exceed 7%. There exists an almost linear relationship between the carbon content and the surface hardness of either pre-test or post-test. It is found that the post-test RCSH of all specimens is much bigger than the pre-test RCSH. This is attributed to the work hardening of materials during testing to some extent.

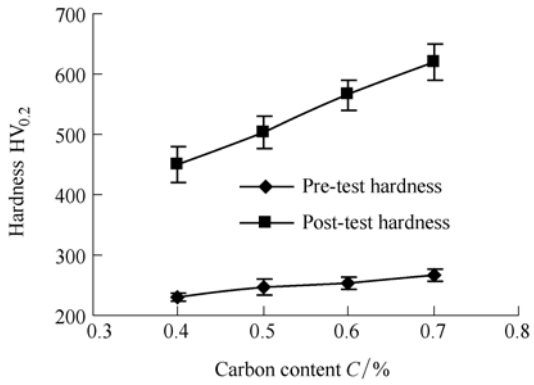

Fig. 9. Variation of pre-test and post-test hardness as function of carbon content

To clarify the effect of the carbon content on the increase in the RCSH, the ratio of the difference between the post-test and pre-test hardness values to the pre-test hardness is defined as hardness increase ratio. The relationship of hardness increase ratio, wear volume and carbon content is shown in Fig. 10. Obviously, the RCSH increase ratio increases with the carbon content of wheel roller. In general, the ability of work hardening can be represented by RCSH increase ratio[14]. So, it can be inferred that the ability of work hardening would be enhanced by the increase in carbon content of materials. As a result, the wear-resistance of wheel roller increases with the carbon content of materials. Therefore, the curves in Fig. 10 exhibit a decrease in wear volume with increase of the carbon content of wheel materials.

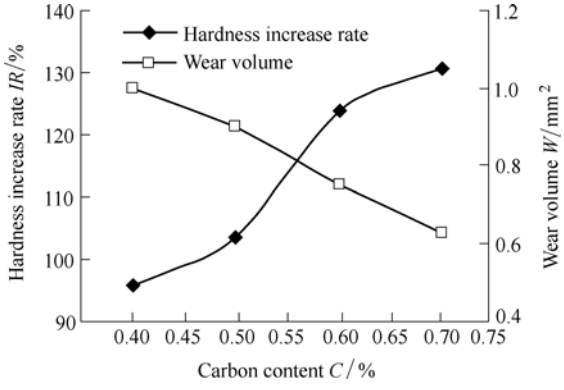

Fig. 10. Variations of hardness increase rate and wear volume as function of carbon content (p=2 400 N)

The SEM micrographs of wear scar of wheel roller with different carbon contents at the creep ratio of −2.3% are shown in Fig. 11. A significant influence of carbon content is found on the rolling wear behavior of wheel material. When the carbon content is low, the worn surface is remarkably smooth accompanied by some very small debris (Fig. 11(a)). With the carbon content increasing, obvious delamination and adhesive wear appear on the worn surfaces (Figs. 11(b) and 11(c)). Large debris and spalling are found on the worn surface when the carbon content increases to 0.7% (Fig. 11(d)).

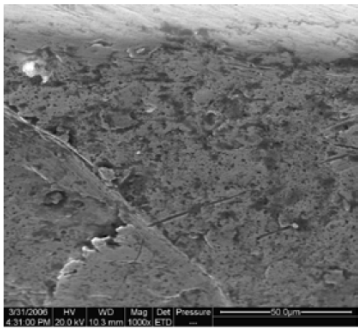

(a) C-0.4%

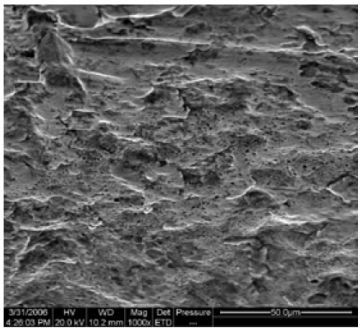

(b) C-0.5%

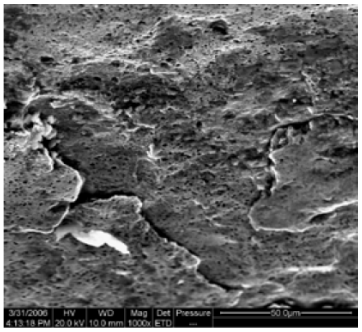

(c) C-0.6%

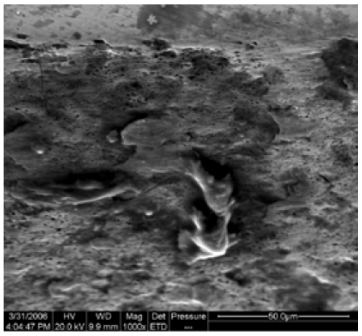

(d) C-0.7%

Fig. 11. SEM micrographs of wear scar of wheel roller with different carbon contents (p=2 400 N)

It is observed in Fig. 12(a) that the plastic deformation is intensive for the wheel roller with lower carbon content. Moreover, the wear volume is big at carbon content 0.4%. Therefore, the wear surface is smooth and no obvious spalling occurs (Fig. 11(a)). With the carbon content increasing, the fatigue microcrack is easily initiated in both the surface and the subsurface due to the repeated friction (Fig. 12(b)). So, wear debris appears on the worn surface, and then spalling damage occurs.

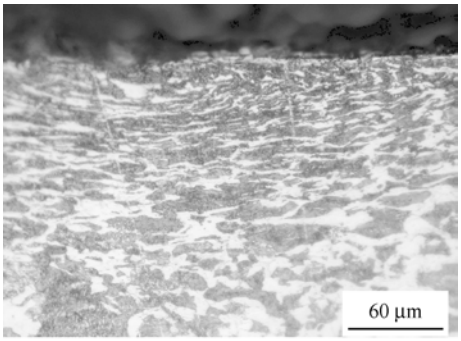

(a) C-0.4%

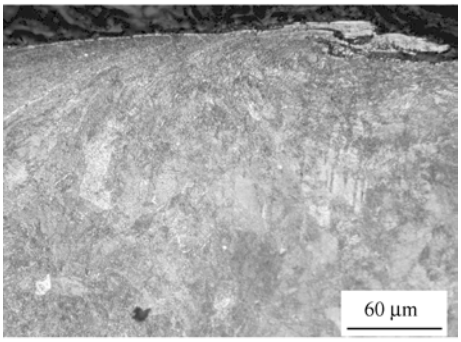

(b) C-0.7%

Fig. 12. Plastic deformation of transverse section of wheel roller (p=2 400 N)

In sum, our research indicates that the creep ratio and carbon content are two significant factors in the rolling wear and spalling behaviors of railway wheel. To some extent, the spalling damage of railway wheel results mainly from rolling contact fatigue. So, some measures could be taken to protect the wheel roller from spalling damage. Firstly, the brake forces in curve and the friction force between wheel and rail should be lowered as far as possible so as to limit the creep ratio of wheel/rail system. Furthermore, an important point to be kept in mind is that appropriate contact between wheel and rail is needed, especially for high-speed railway, because poor contact between wheel and rail in curve would make the wheel tread suffer from high contact stress[15–16]. Secondly, the yield strength, fatigue strength and fatigue-resistance of wheel materials should be enhanced. Our study implies that decreasing the carbon content of wheel materials can alleviate spalling damage of railway wheel, but inevitably increase wear volume of material. It is reported that alloying some elements, such silicon, cobalt, and so on, into wheel materials could alleviate the spalling of steel without the decrease in its wear-resistance[17]. Therefore,

especially for high-speed railway, a developing tendency of railway wheel material is to decrease the carbon content accompanied by alloying the materials.

4 Conclusions

(1) The wear and spalling behaviors of railway wheel depend strongly on the creep ratio and normal load between wheel and rail. With the creep ratio increasing, the wear mechanisms of wheel roller change from abrasion into adhesion and fatigue, and then spalling occurs on the rolling contact surface. Wear volume increases not only rapidly with the creep ratio but also proportionally with normal load.

(2) The carbon content of wheel materials can significantly affect the rolling wear behavior. A decrease in the carbon content may alleviate spalling damage but cause a linear increase in the wear volume of wheel roller.

References

[1] EKBERG A, KABO E. Fatigue of railway wheels and rails under rolling contact and thermal loading-an overview[J]. *Wear*, 2005, 258(7–8): 1 288–1 300.

[2] SUN J, SAWLEY K J, STONE D H. Progress in the reduction of wheel spalling[C]//*Proceeding of the 12th International Wheelset Congress*, Qingdao, China, September 21–25, 1998: 18–29.

[3] TAKIKAWA M, IRIYA Y. Laboratory simulations with twin-disc machine on head check[J]. *Wear*, 2008, 265(9–10): 1 300–1 308.

[4] JIN Xuesong, WEN Zefeng, WANG Kaiyun, et al. Effect of a scratch on curved rail on initiation and evolution of rail corrugation[J]. *Tribology International*, 2004, 37(5): 385–394.

[5] STONE D H, MOYER G J. Wheel shelling and spalling-an interpretive review[J]. *Rail Transportation*, 1989, 5(1): 9–30.

[6] MAKINO T, YAMANOTO M, FUJIMURA T. Effect of material on spalling properties of railroad wheels[J]. *Wear*, 2002, 253(1–2): 284–290.

[7] KALOUSEK J. Wheel/rail damage and its relationship to track curvature[J]. *Wear*, 2005, 258(7–8): 1 330–1 335.

[8] AHLSTROM J, KARLSSON B. Microstructural evaluation and interpretation of the mechanically and thermally affected zone under railway wheel flats[J]. *Wear*, 1999, 232(1): 1–14.

[9] SAKAMOTO H, HIRAKAWA K, TOYAMA K, et al. Simulation test on tread shelling of railroad wheel[J]. *Rail Transportation*, 1996, 12(2): 73–78.

[10] JIN Xuesong, LIU Qiyue. *Tribology of wheel and rail system*[M]. Beijing: China Railway Press, 2004. (in Chinese)

[11] WALLENTIN M, BJARNEHED H L, LINDENS R. Cracks around railway wheel flats exposed to rolling contact loads and residual stresses[J]. *Wear*, 2005, 258(7–8): 1 319–1 329.

[12] LIU Qiyue, JIN Xuesong, ZHOU Zhongrong. An investigation of friction characteristic of steels under rolling–sliding condition[J]. *Wear*, 2005, 259(1–6): 439–444.

[13] DETERS L, PROKSCH M. Friction and wear testing of rail and wheel material[J]. *Wear*, 2005, 258(7–12): 981–991.

[14] UEDA M, UHCINO K, KOBAYASHI A. Effects of carbon content on wear property in pearlitic steels[J]. *Wear*, 2002, 253(1–2): 107–113.

[15] DONZELLA G, MAZZU A, PTTROGALLI C. Competition between wear and rolling contact fatiuge at the wheel-rail interface: some experimental evidence on rail steel[J]. *Proc. ImechE Part F: Rail and Rapid Transit*, 2009, 223(1): 31–44.

[16] EKBERG A, SOTKOVSZKI P. Anisotropy and rolling contact fatigue of railway wheels[J]. *International Journal of Fatigue*, 2001, 23(1): 29–43.

[17] HARUO S, KAZUO T, KENJI H. Fracture toughness of medium-high carbon steel for railroad wheel[J]. *Materials Science and Engineering*, 2000, 285(1–2): 288–292.

Biographical notes

WANG Wenjian, born in 1980, is currently an associate researcher at *Tribology Research Institute, Southwest Jiaotong University, China*. He received his PhD degree from *Southwest Jiaotong University, China*, in 2008. His research interests include the tribology of wheel/rail system and rail grinding technique.
Tel: +86-28-87634304; E-mail: wwj527@163.com

GUO Jun, born in 1972, is currently a researcher at *Tribology Research Institute, Southwest Jiaotong University, China*. He received his PhD degree from *Southwest Jiaotong University, China*, in 2007. His research interests include the tribology of wheel/rail.
E-mail: guojun@home.swjtu.edu.cn

LIU Qiyue, born in 1964, is currently a professor at *Tribology Research Institute, Southwest Jiaotong University, China*. He received his PhD degree from *Southwest Jiaotong University, China*, in 1999. His research interests include the wear and damage of wheel/rail materials.
E-mail: liuqy@swjtu.cn